Key comparison BIPM.RI(I)-K9 of the absorbed dose to water standards of the LNE-LNHB, France, and the BIPM in medium-energy x-rays

D T Burns[1], C Kessler[1] and B Rapp[2]

[1] Bureau International des Poids et Mesures (BIPM), Pavillon de Breteuil, F-92310 Sèvres
[2] CEA-LIST Laboratoire National Henri Becquerel, CEA Saclay, 91191 Gif sur Yvette, France

Abstract A key comparison has been made between the absorbed dose to water standards of the LNE-LNHB, France, and the BIPM in the medium-energy x-ray range. The results show the standards to be in general agreement at the level of the expanded ($k = 2$) uncertainty of the comparison of 2 parts in 10^2. The results are presented in terms of degrees of equivalence for entry in the BIPM key comparison database.

1. Introduction

An indirect comparison has been made between the absorbed dose to water standards of the Laboratoire National Henri Becquerel (LNE-LNHB), France, and the Bureau International des Poids et Mesures (BIPM) in the x-ray range from 100 kV to 250 kV. Two cavity ionization chambers were used as transfer instruments. The measurements at the BIPM took place in October 2018 using the reference conditions recommended by the CCRI (CCEMRI 1972). Final information was supplied by the LNE-LNHB in November 2019. Note that the BIPM standard includes the recommendations of ICRU Report 90 (ICRU 2016) as documented in Burns and Kessler (2018) and Burns *et al.* (2017).

2. The BIPM standard for absorbed dose to water

At the BIPM, the absorbed dose to water is derived from the air-kerma determined using a free-air ionization chamber standard with measuring volume V. The air-kerma rate is derived using the relation

$$\dot{K}_{\mathrm{air}} = \frac{I}{\rho_{\mathrm{air}}V} \, \frac{W_{\mathrm{air}}}{e} \, \frac{1}{1-g_{\mathrm{air}}} \prod_i k_i \, , \tag{1}$$

where ρ_{air} is the density of air under reference conditions, I is the ionization current under the same conditions, W_{air} is the mean energy expended by an electron of charge e to produce an ion pair in air, g_{air} is the fraction of the initial electron energy lost through radiative processes in air, and $\prod k_i$ is the product of the correction factors to be applied to the standard.

The values used for the physical constants ρ_{air} and W_{air}/e are given in Table 1. For use with this dry-air value for ρ_{air}, the ionization current I must be corrected for humidity and for the difference between the density of the air of the measuring volume at the time of measurement and the value given in the table.

Table 1. Physical constants used in the determination of the BIPM air-kerma rate

Constant	Value	u_i[a]
ρ_{air}[b]	1.2045 kg m^{-3}	0.0001
W_{air}/e	33.97 J C^{-1}	0.0035[c]

[a] u_i is the relative standard uncertainty.
[b] Density of dry air at $T_0 = 293.15$ K and $P_0 = 101.325$ kPa adopted at the BIPM.
[c] Revised uncertainty adopted by the CCRI from January 2018.

The BIPM air-kerma standard FAC-M-01 is described in Boutillon (1978) and the changes made to certain correction factors in Burns (2004), Burns *et al.* (2009), Burns and Kessler (2018) and the references therein. The main dimensions, measuring volume and polarizing voltage are given in Table 2 and the correction factors k_i (and g_{air}) and their associated uncertainties in Table 3.

Table 2. Main characteristics of the BIPM air-kerma standard

Standard	BIPM FAC-M-01
Aperture diameter / mm	9.939
Air path length / mm	281.5
Collecting length / mm	60.004
Electrode separation / mm	180
Collector width / mm	200
Measuring volume V / mm^3	4655.4
Polarizing voltage / V	4000

Table 3. Correction factors for the BIPM air-kerma standard

Radiation quality	100 kV	135 kV	180 kV	250 kV	u_{iA}	u_{iB}
Air attenuation k_a [a]	1.0099	1.0065	1.0055	1.0047	0.0002	0.0001
Photon scatter k_{sc}	0.9952	0.9959	0.9964	0.9974	-	0.0003
Fluorescence k_{fl}	0.9985	0.9992	0.9994	0.9999	-	0.0003
Electron loss k_e [b]	1.0000	1.0015	1.0047	1.0085	-	0.0005
Initial ionization and W_{air} $k_{ii}k_W$ [b]	0.9980	0.9980	0.9981	0.9986	-	0.0005
Ion recombination k_s	1.0010	1.0010	1.0010	1.0010	0.0002	0.0001
Polarity k_{pol}	1.0002	1.0002	1.0002	1.0002	0.0001	-
Field distortion k_d	1.0000	1.0000	1.0000	1.0000	-	0.0007
Diaphragm correction k_{dia}	0.9995	0.9993	0.9991	0.9980	-	0.0003
Wall transmission k_p	1.0000	1.0000	0.9999	0.9988	0.0001	-
Humidity k_h	0.9980	0.9980	0.9980	0.9980	-	0.0003
Radiative loss $1 - g_{air}$	0.9999	0.9999	0.9998	0.9997	-	0.0001

[a] Values for 293.15 K and 101.325 kPa; each measurement is corrected using the air density measured at the time.
[b] The combined correction factor $k_{ii}k_W$ is described in Burns (2017) and the references therein. The stated values and uncertainties are taken from the same report.

The report of Burns *et al.* (2017) describes the conversion from the air-kerma rate at the reference distance of 1200 mm in air, for a field of diameter 98 mm at this distance, to the rate of absorbed dose to water at this distance at a depth of 2 g cm^{-2} in a cubic water phantom of side length 20 cm. For this dose conversion, reference ionization chambers were positioned in air and

at a depth of 2 g cm^{-2} in water. The depth is evaluated taking into account the PMMA window of thickness 1.677 mm and nominal density 1.19 g cm^{-3}, and the water density of 0.9982 g cm^{-3} at 20 °C.

The rate of absorbed dose to water on the central axis at the depth of 2 g cm^{-2} in the BIPM phantom is derived from the air-kerma rate given by equation (1) using the relation

$$\dot{D}_w = \overline{C}_{w,air}\,\dot{K}_{air}. \tag{2}$$

The conversion factor $\overline{C}_{w,air}$ is the mean for a series of reference ionization chambers; for each chamber it is evaluated as

$$C_{w,air} = \frac{Q_w}{Q_{air}} k_{rn} \left(\frac{D_w/D_{cav,w}}{K_{air}/D_{cav,air}} \right)_{MC}, \tag{3}$$

where Q_w/Q_{air} is the measured charge ratio water-to-air for a given reference chamber. The factor in parenthesis, calculated using Monte Carlo (MC) methods, is essentially a ratio of absorbed-dose and air-kerma 'calibration coefficients' for the given reference chamber type, $D_{cav,w}$ and $D_{cav,air}$ representing the mean absorbed dose to the air of the chamber cavity when in water and air, respectively. The measured non-uniformity factor k_{rn} corrects the charge reading in water such that $\dot{D}_w$ represents the central-axis dose rate.

The BIPM reference values for $\overline{C}_{w,air}$ and their relative standard uncertainty are taken from Burns *et al.* (2017) and given in Table 4.

Table 4. The conversion factor from air kerma to absorbed dose to water for the BIPM standard

	100 kV	135 kV	180 kV	250 kV	u_{iA}	u_{iB}
$\overline{C}_{w,air}$	1.1840	1.4294	1.4429	1.3673	0.0013	0.0040

3. The LNE-LNHB standard for absorbed dose to water

The LNE-LNHB primary standard for absorbed dose to water is a water calorimeter as described in Rapp *et al.* (2013). The absorbed dose to water D_w is determined from the radiation-induced temperature rise ΔT using the equation

$$D_w = \Delta T\, c_p\, (1-h)^{-1} k_p\, k_c\, k_\rho\, k_d, \tag{4}$$

where c_p is the specific heat capacity of water at 4 °C (4204.8 J kg^{-1} K^{-1}), h is the chemical heat defect, which for nitrogen-saturated water is taken to be unity with an uncertainty of 3 parts in 10^3, k_p is the radiation field perturbation correction factor, k_c is the thermal conduction correction factor, k_ρ is the water density correction factor and k_d is the depth correction factor. The values of these factors used for the present comparison are given in Table 5.

4. The transfer instruments

4.1 Determination of the calibration coefficient for a transfer instrument

The absorbed dose to water calibration coefficient $N_{D,w}$ for a transfer instrument is given by the relation

$$N_{D,w} = \frac{\dot{D}_w}{I_{tr}}, \tag{5}$$

where $\dot{D}_w$ is the rate of absorbed dose to water determined by the standard and I_{tr} is the ionization current measured by the transfer instrument and the associated current-measuring system. The

current I_{tr} is corrected to the standard conditions of air temperature, pressure and relative humidity chosen for the comparison ($T = 293.15$ K, $P = 101\,325$ kPa and $h = 50$ %).

To derive a comparison result from the calibration coefficients $N_{D,w,BIPM}$ and $N_{D,w,NMI}$ measured, respectively, at the BIPM and at a national metrology institute (NMI), differences in the radiation qualities must be taken into account. Normally, each quality used for the comparison has the same nominal generating potential at each institute, but the half-value layers (HVLs) may differ. A radiation quality correction factor k_Q is derived for each comparison quality Q. This corrects the calibration coefficient $N_{D,w,NMI}$ determined at the NMI into one that applies at the 'equivalent' BIPM quality and is derived by interpolation in terms of log(HVL). The comparison result at each quality is then taken as

$$R_{D,w,NMI} = \frac{k_Q N_{D,w,NMI}}{N_{D,w,BIPM}}. \tag{6}$$

In practice, the half-value layers normally differ by only a small amount and k_Q is close to unity.

Table 5. Correction factors for the LNE-LNHB standard at the CCRI radiation qualities

	100 kV	135 kV	180 kV	250 kV	u_{iA}	u_{iB}
Perturbation k_p	1.0549	1.0342	1.0263	1.0164	-	0.0012
Conduction k_c	1.0089	1.0027	0.9996	1.0023	-	0.003 [a]
Density k_ρ	1.00044	1.00025	1.00021	1.00019	-	0.00002
Depth k_d	0.9965	0.9979	0.9981	0.9983	-	0.0001

[a] Approximate value. The actual values are 0.0035, 0.0031, 0.0028 and 0.0025 for the radiation qualities 100 kV, 135 kV, 180 kV and 250 kV, respectively.

4.2 Details of the transfer instruments

Two Farmer-type waterproof thimble chambers belonging to the LNE-LNHB were used as transfer instruments for the comparison. Each chamber was positioned directly in water, without a waterproof sleeve, at the depth where the absorbed dose rate is known, nominally 2 g cm^{-2}. The main characteristics of the chambers are given in Table 6.

Table 6. Main characteristics of the transfer chambers

Chamber type	PTW 30013	
Serial number	5919	8859
External diameter / mm	6.90	6.90
Wall material	0.335 mm PMMA + 0.09 mm graphite	
Wall thickness	0.0565 g cm^{-2}	
Nominal volume / cm^3	0.6	
Polarizing potential / V	+300[a]	

[a] Potential applied to the outer electrode.

5. Calibration at the BIPM

5.1 The BIPM irradiation facility and reference radiation qualities

The BIPM medium-energy x-ray laboratory houses a high-stability generator and a tungsten-anode x-ray tube with a 3 mm beryllium window. An aluminium filter of thickness 2.228 mm is added (for all radiation qualities) to compensate for the decrease in attenuation that occurred when the original BIPM x-ray tube (with an aluminium window of approximately 3 mm) was replaced in June 2004. Two voltage dividers monitor the tube voltage and a voltage-to-frequency converter combined with data transfer by optical fibre measures the anode current. No transmission monitor is used. For a given radiation quality, the standard uncertainty of the distribution of repeat air-kerma rate determinations over many months is typically 3 parts in 10^4. Repeat calibrations in water using reference ionization chambers over several months preceding the present comparison show a standard deviation of around 2 parts in 10^4. The radiation qualities used in the range from 100 kV to 250 kV are those recommended by the CCRI (CCEMRI 1972) and details of their realization at the BIPM are given in Table 7.

Table 7. Characteristics of the BIPM reference radiation qualities

Radiation quality	100 kV	135 kV	180 kV	250 kV
Generating potential / kV	100	135	180	250
Inherent Be filtration / mm	3	3	3	3
Additional Al filtration / mm	3.431	2.228	2.228	2.228
Additional Cu filtration / mm	-	0.232	0.485	1.570
Al HVL / mm	4.030	-	-	-
Cu HVL / mm	0.149	0.489	0.977	2.484
$(\mu/\rho)_{air}$ / cm^2 g^{-1}	0.290	0.190	0.162	0.137
$\dot{K}_{air,BIPM}$ / mGy s^{-1}	0.50	0.50	0.50	0.50
$\dot{D}_{w,BIPM}$ / mGy s^{-1}	0.59	0.71	0.72	0.68

The reference distance at the BIPM is 1200 mm from the radiation source, where the field diameter is 98 mm. The irradiation area is temperature controlled in the range from 20 °C to 21 °C and is stable over the duration of a calibration to better than 0.1 °C. Three calibrated thermistors measure the temperature of the ambient air, the air inside the BIPM standard (which is controlled at 25 °C) and the water temperature at the height of the beam axis. Air pressure is measured by means of a calibrated barometer. The relative humidity is controlled within the range from 40 % to 50 % and consequently no humidity correction is applied to the current measured using transfer instruments.

5.2 Measurements using the BIPM standard

The reference plane for the BIPM free-air chamber standard was positioned at the reference distance (1200 mm), with a reproducibility of 0.03 mm. The standard was aligned on the beam axis to an estimated uncertainty of 0.1 mm.

During the calibration of the transfer chambers, measurements using the standard were made using positive polarity only. A correction factor of 1.00015 is applied to correct for the known polarity effect in the standard. The leakage current, relative to the ionization current, was measured to be around 1 part in 10^4.

5.3 Transfer chamber positioning and calibration at the BIPM

Transfer chambers are calibrated at the BIPM in the cubic water phantom of side length 20 cm used for the primary determination of the water absorbed-dose rate, for which the entrance window is PMMA of thickness 1.677 mm. With the phantom lowered below the beam axis, the reference point for each transfer chamber was positioned at the reference distance (1200 mm from the radiation source), with a reproducibility of 0.01 mm. The reference point for each chamber (taken to be 13 mm from the tip) was aligned on the beam axis to an estimated uncertainty of 0.1 mm. The filled water phantom was then raised and the outer surface of the front face positioned 19.71 mm closer to the source, corresponding to 2.00 g cm^{-2} when account is taken of the window density (nominally 1.19 g cm^{-3}) and the water density (0.9982 g cm^{-3} at 20 °C), with a reproducibility of 0.01 mm.

The leakage current was measured before and after each series of ionization current measurements and a correction made using the mean value. The relative leakage current for each transfer chamber was typically below 1 part in 10^4.

For the calibration of each transfer chamber at each radiation quality, a set of seven measurements was made, each measurement with integration time 60 s. The relative standard uncertainty of the mean ionization current for each set was below 2 parts in 10^4 for both chambers. Repeat calibrations for both chambers at all radiation qualities, after re-positioning in the water phantom, showed a standard deviation of typically 5 parts in 10^4 (higher than the reproducibility of the BIPM reference chambers of 2 parts in 10^4 noted in Section 5.1). Based on these measurements, an uncertainty component of 5 parts in 10^4 is introduced in Table 11 to account for the short-term reproducibility of the chamber calibration coefficients at the BIPM.

6. Calibration at the LNE-LNHB

6.1 The LNE-LNHB irradiation facility and reference radiation qualities

The medium-energy x-ray facility of the LNE-LNHB comprises a constant-potential generator and a tungsten-anode x-ray tube with an inherent filtration of 3 mm beryllium. The generator was allowed to stabilize for more than one hour before measurements. No monitor chamber was used. Output stability is around 5 parts in 10^4 and the reproducibility of the air-kerma determinations is around 8 parts in 10^4. The characteristics of the LNE-LNHB realization of the CCRI comparison qualities (CCEMRI 1972) are given in Table 8.

Table 8. Characteristics of the LNE-LNHB reference radiation qualities

Radiation quality	100 kV	135 kV	180 kV	250 kV
Generating potential / kV	100	135	180	250
Additional Al filtration / mm	3.402	2.498	2.968	2.968
Additional Cu filtration / mm	-	0.225	0.467	1.624
Al HVL [a] / mm	4.038	-	-	-
Cu HVL [a] / mm	-	0.490	0.974	2.477
$\dot{D}_{w,\text{LNE-LNHB}}$ / mGy s^{-1}	7.7	9.4	6.7	8.1

[a] As determined at the distance of 1200 mm used for the LNE-LNHB air-kerma standard.

To obtain a higher absorbed-dose rate suitable for calorimetry, the reference distance at the LNE-LNHB is 530 mm from the radiation source, where the field size is 104 mm by 104 mm. The irradiation area at the LNE-LNHB is temperature controlled at around 20 °C and is stable over the duration of a calibration to better than 0.5 °C. A calibrated resistance temperature detector (RTD) positioned in the water phantom measures the temperature at the height of the beam axis. Air pressure is measured by means of a calibrated barometer. The relative humidity is controlled within the range from 35 % to 65 % and consequently no humidity correction is applied to the current measured using the transfer instruments.

6.2 Measurements using the LNE-LNHB standard

The rates of absorbed dose to water for the CCRI qualities at the LNE-LNHB were measured using the water calorimeter in June 2014. Two independent thermistor probes were used for the measurements. Typically 30 individual measurements were performed for each beam and the resulting statistical uncertainty of the temperature rise was in the range from 0.45 % to 0.88 % depending on radiation quality.

During the same period, two Farmer-type reference ionization chambers (one NE 2571 and one PTW 30013) were calibrated directly against the water calorimeter and these reference chambers were used to cross-calibrate the transfer chambers for the present comparison.

6.3 Transfer chamber positioning and calibration at the LNE-LNHB

Ionization chambers are calibrated at the LNE-LNHB in a cubic water phantom of side length 30 cm with a quartz entrance window 0.08 cm in thickness and 12 cm in diameter. This phantom is designed to reproduce the water calorimeter phantom in term of materials and dimensions, with in addition a support for positioning ionization chambers. Chambers are positioned at a depth of 2 cm (comprising 0.08 cm of quartz and 1.92 cm of water), corresponding to the reference depth for calorimeter measurements. Positioning at this depth is achieved using a suitable gauge block placed inside the phantom, in contact with the quartz window and the surface of the chamber. Gauge blocks are machined for a given ionization chamber type with a thickness that takes into account the nominal external radius of the chamber type. To take into account small variations in radius for individual chambers, a correction factor for the exact positioning of the chambers is applied, which for the present comparison ranges from 0.9991(17) to 0.9996(10) depending on radiation quality.

The leakage current was measured before and after each series of ionization current measurements and a correction made using the mean value. The relative leakage current for each transfer chambers was typically less than 2 parts in 10^4.

For the calibration of each transfer chamber at each radiation quality, three sets of 60 measurements were made, each measurement with an integration time of 5 s. The relative standard uncertainty of the mean ionization current for each set was typically 3 parts in 10^4 for both chambers. Repeat calibrations for both chambers at all radiation qualities, including re-positioning in the water phantom, showed a standard deviation lower than 1 part in 10^3. Based on these measurements, an uncertainty component of 1 part in 10^3 is introduced in Table 12 to account for reproducibility of the chamber calibration coefficients at the LNE-LNHB.

7. Additional corrections to transfer chamber measurements

7.1 Ion recombination, polarity, beam non-uniformity and field size

As can be seen from Tables 7 and 8 the absorbed-dose rates at the LNE-LNHB are ten to twelve times greater than those at the BIPM. Based on previous measurements in 50 kV x-rays at the BIPM the effect of this for Farmer-type thimble chambers is estimated to be around 1.5 parts

in 10^3. No corrections are applied for ion recombination and a corresponding uncertainty of 1.5 parts in 10^3 is included in Table 13. Each transfer chamber was used with the same polarity at each laboratory and no corrections are applied for polarity effects in the transfer chambers.

For thimble-type chambers, the radial non-uniformity correction determined at 2 g cm^{-2} in the BIPM reference beams is around 3 parts in 10^3. As this correction is likely to be similar at the two laboratories, no corrections are applied for non-uniformity but an uncertainty component of 8 parts in 10^4 is included in Table 13. As the field sizes at the LNE-LNHB and the BIPM are each close to 100 mm, no field-size corrections are applied.

7.2 *Radiation quality correction factors k_Q*

As noted in Section 4.1, slight differences in radiation qualities may require a correction factor k_Q. From Tables 6 and 8 it is evident that the radiation qualities at the LNE-LNHB and the BIPM are closely matched and the k_Q value is taken to be unity for all radiation qualities, with a corresponding uncertainty of 2 parts in 10^4 included in Table 13.

8. Comparison results

The calibration coefficients $N_{D,w,\text{LNE-LNHB}}$ and $N_{D,w,\text{BIPM}}$ for the transfer chambers are presented in Table 9 and the comparison results $R_{D,w,\text{LNE-LNHB}}$ evaluated according to Equation (6) given in Table 10.

Table 9. Calibration coefficients for the transfer chambers

Radiation quality	100 kV	135 kV	180 kV	250 kV
Transfer chamber PTW 30013-5919				
$N_{D,w,\text{LNE-LNHB}}$ / Gy μC^{-1}	48.905	51.246	51.167	53.188
$N_{D,w,\text{BIPM}}$ / Gy μC^{-1}	50.027	51.298	51.958	52.784
Transfer chamber PTW 30013-8859				
$N_{D,w,\text{LNE-LNHB}}$ / Gy μC^{-1}	49.248	51.597	51.492	53.535
$N_{D,w,\text{BIPM}}$ / Gy μC^{-1}	50.349	51.661	52.322	53.157

Table 10. Comparison results

Radiation quality	100 kV	135 kV	180 kV	250 kV
$R_{D,w,\text{LNE-LNHB}}$ using PTW30013-5919	0.9776	0.9990	0.9848	1.0077
$R_{D,w,\text{LNE-LNHB}}$ using PTW30013-8859	0.9781	0.9988	0.9841	1.0071
s_{tr}	0.0003	0.0001	0.0005	0.0004
Final $R_{D,w,\text{LNE-LNHB}}$	**0.9779**	**0.9989**	**0.9845**	**1.0074**
Results in EURAMET.RI(I)-S13	*0.9787*	*1.0000*	*0.9850*	*1.0096*

For each quality, the final result in bold in Table 10 is evaluated as the mean for the two transfer chambers. The corresponding uncertainty s_{tr} is the standard uncertainty of this mean arising from the difference in the results for the two transfer chambers[1]. The r.m.s. value of s_{tr} for the four qualities, $s_{tr,comp} = 0.0004$, is a global representation of the comparison uncertainty arising from the transfer chambers and is included in Table 13. Also given in Table 10 are the LNE-LNHB results relative to the BIPM obtained in the EURAMET.RI(I)-S13 comparison (Büermann *et al.* 2016). It is these results that currently appear in the BIPM key comparison database (KCDB 2019).

9. Uncertainties

The uncertainties associated with the BIPM primary standard and the calibrations of the transfer chambers are listed in Table 11 and those for the LNE-LNHB in Table 12. The combined standard uncertainties for the comparison results $R_{D,w,LNE-LNHB}$ are presented in Table 13.

Table 11. Uncertainties associated with the BIPM standard and transfer chamber calibrations

Relative standard uncertainty	u_{iA}	u_{iB}
Air-kerma rate		
Positioning of standard	0.0001	0.0001
Ionization current	0.0002	0.0002
Volume	0.0001	0.0005
Correction factors (excl. k_h)	0.0003	0.0011
Humidity k_h	-	0.0003
Physical constants	-	0.0035
Absorbed-dose conversion		
$\overline{C}_{w,air}$	0.0013	0.0040
$\dot{D}_{w,BIPM}$	**0.0014**	**0.0055**
Transfer chamber calibrations		
Positioning of chamber	-	0.0002
I_{tr}	0.0002	0.0002
Reproducibility	0.0005	-
$N_{D,w,BIPM}$	**0.0015**	**0.0055**

---

[1] The standard uncertainty of the mean is evaluated as the standard deviation of the population divided by $(n–1.4)$, found empirically to be a better choice than $(n–1)$ to estimate the standard uncertainty for low values of n.

Table 12. Uncertainties associated with the LNE-LNHB standard and transfer chamber calibrations

Radiation quality	100 kV		135 kV		180 kV		250 kV	
Relative standard uncertainty	u_{iA}	u_{iB}	u_{iA}	u_{iB}	u_{iA}	u_{iB}	u_{iA}	u_{iB}
Absorbed-dose rate								
Temperature probe positioning	-	0.0009	-	0.0007	-	0.0006	-	0.0006
Temperature probe calibration	-	0.001	-	0.001	-	0.001	-	0.001
Reproducibility of ΔT	0.0088	-	0.0045	-	0.0072	-	0.0047	-
Irradiation time	0.0003	-	0.0003	-	0.0003	-	0.0003	-
Correction factors (Table 5)	-	0.0037	-	0.0033	-	0.0030	-	0.0028
Specific heat capacity c_p	-	0.001	-	0.001	-	0.001	-	0.001
Heat defect $(1-h)^{-1}$	-	0.003	-	0.003	-	0.003	-	0.003
$\dot{D}_{w,\text{LNE-LNHB}}$	**0.0088**	**0.0050**	**0.0045**	**0.0047**	**0.0072**	**0.0045**	**0.0047**	**0.0044**
Transfer chamber calibrations								
Positioning of chamber	-	0.0017	-	0.0011	-	0.0010	-	0.0010
I_{tr}	0.0003	0.0007	0.0003	0.0007	0.0003	0.0007	0.0003	0.0007
Reproducibility	0.001	-	0.001	-	0.001	-	0.001	-
$N_{D,w,\text{LNE-LNHB}}$	**0.0089**	**0.0053**	**0.0046**	**0.0049**	**0.0073**	**0.0047**	**0.0048**	**0.0046**

Table 13. Uncertainties associated with the comparison results

Radiation quality	100 kV	135 kV	180 kV	250 kV
$N_{D,w,\text{LNE-LNHB}}$ / $N_{D,w,\text{BIPM}}$	0.0118	0.0088	0.0104	0.0088
Ion recombination	0.0015			
Radial non-uniformity	0.0008			
Transfer chambers $s_{tr,comp}$	0.0004			
k_Q	0.0002			
$R_{D,w,\text{LNE-LNHB}}$	**0.012**	**0.009**	**0.011**	**0.009**

10. Discussion

The comparison results presented in Table 10 show the LNE-LNHB and BIPM standards to be in general agreement at the level of the expanded ($k = 2$) uncertainty of the comparison of 2 parts in 10^2. No clear trend with radiation quality is evident in the results, but rather scatter around a mean value of 0.992 with a standard deviation of 1.3 parts in 10^2. It is clear that this significant scatter does not come from the transfer chamber calibrations as the two chambers give similar

results at the level of 4 parts in 10^4. From the shape of the calibration curves $N_{D,w}$ as a function of HVL shown in Figure 1, it is evident that the variations for the LNE-LNHB values arise from underlying statistical variations in the calorimeter standard, as might be expected from the large type A uncertainty for the temperature rise ΔT in Table 12. One can make the same deduction from the close agreement between the present results and those obtained in the EURAMET.RI(I)-S13 comparison, presented in the final row of Table 10. The same underlying calorimeter data have been used for both comparisons.
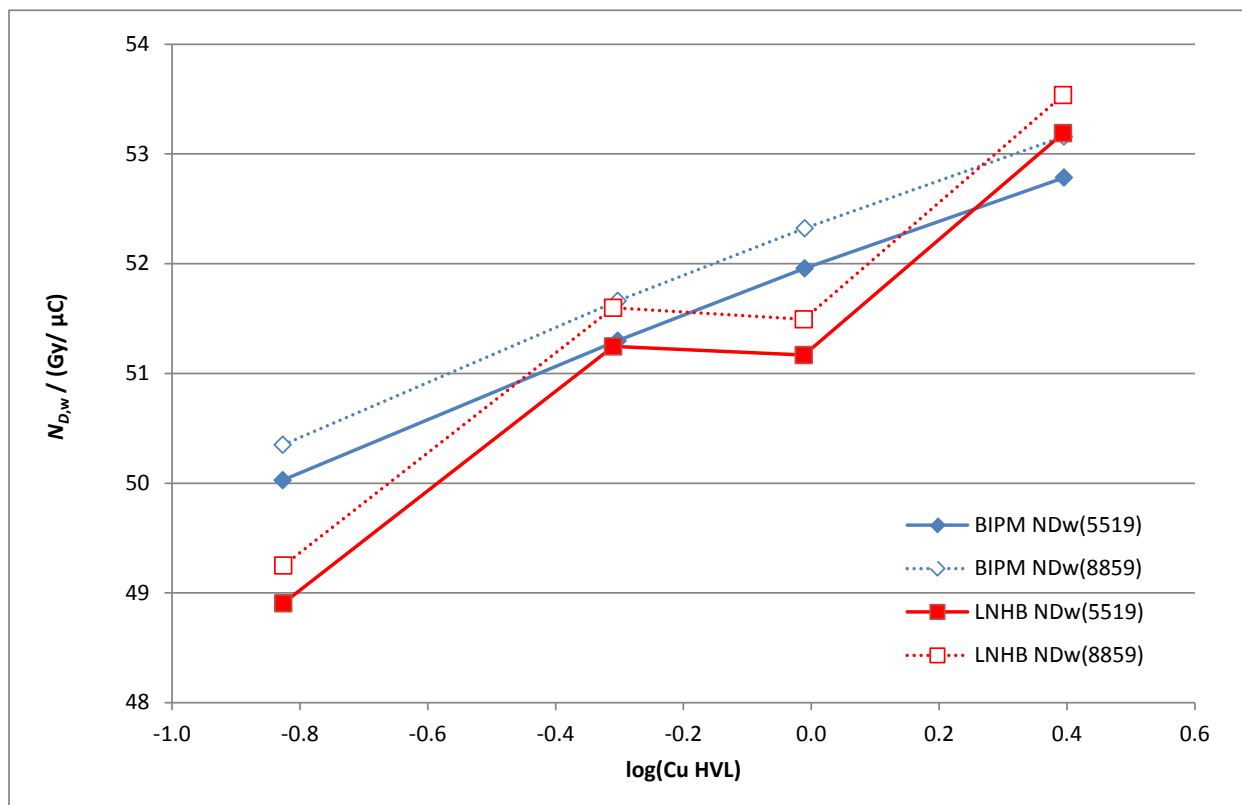

Figure 1. Calibration coefficients for the transfer chambers. For the BIPM results (blue), showing a smooth variation with HVL, the statistical variations are dominated by current measurements (free-air chamber standard and transfer chamber). For the LNE-LNHB results (red), showing greater scatter, the statistical variations are dominated by the calorimeter standard and are correlated for the two transfer chambers because the same calorimeter data are used.

11. Degrees of Equivalence

The analysis of the results of BIPM comparisons for air kerma in medium-energy x-rays in terms of degrees of equivalence is described in Burns (2003). Following a decision of the CCRI in 2017, and in common with all other key comparisons in the series BIPM.R(I), the BIPM determination of the rate of absorbed dose to water is taken as the key comparison reference value, for each of the CCRI radiation qualities. It follows that for each laboratory i having a BIPM comparison result x_i with combined standard uncertainty u_i, the degree of equivalence with respect to the reference value is the relative difference $D_i = (K_i - K_{\text{BIPM},i}) / K_{\text{BIPM},i} = x_i - 1$ and its expanded uncertainty $U_i = 2 u_i$. The results for D_i and U_i, expressed in mGy/Gy are shown in Table 14 and in Figure 2. These include the linked results of the EURAMET.RI(I)-S13 comparison (Büermann *et al.* 2016). Note that these data, while correct at the time of publication of the present report, become out of date as laboratories make new comparisons. The formal results under the CIPM MRA are those available in the BIPM key comparison database (KCDB 2019).

Table 14. Degrees of equivalence. For each laboratory *i*, the degree of equivalence with respect to the key comparison reference value is the difference D_i and its expanded uncertainty U_i. Tables formatted as they appear in the BIPM key comparison database; red indicates participation in BIPM.RI(I)-K9 and blue in EURAMET.RI(I)-S13.

| Lab *i* | 100 kV | | 135 kV | | 180 kV | | 250 kV | |
	D_i /(mGy/Gy)	U_i /(mGy/Gy)	D_i /(mGy/Gy)	U_i /(mGy/Gy)	D_i /(mGy/Gy)	U_i /(mGy/Gy)	D_i /(mGy/Gy)	U_i /(mGy/Gy)
PTB	-6.7	21.4	-11.1	20.2	-9.4	17.8	-5.3	17.8
LNHB	-22.1	23.8	-1.1	18.0	-15.5	21.0	7.4	18.0
ENEA					-7.7	40.0	8.5	40.0
VSL	-5.4	20.7	9.9	19.6	-1.4	19.0	1.9	19.5
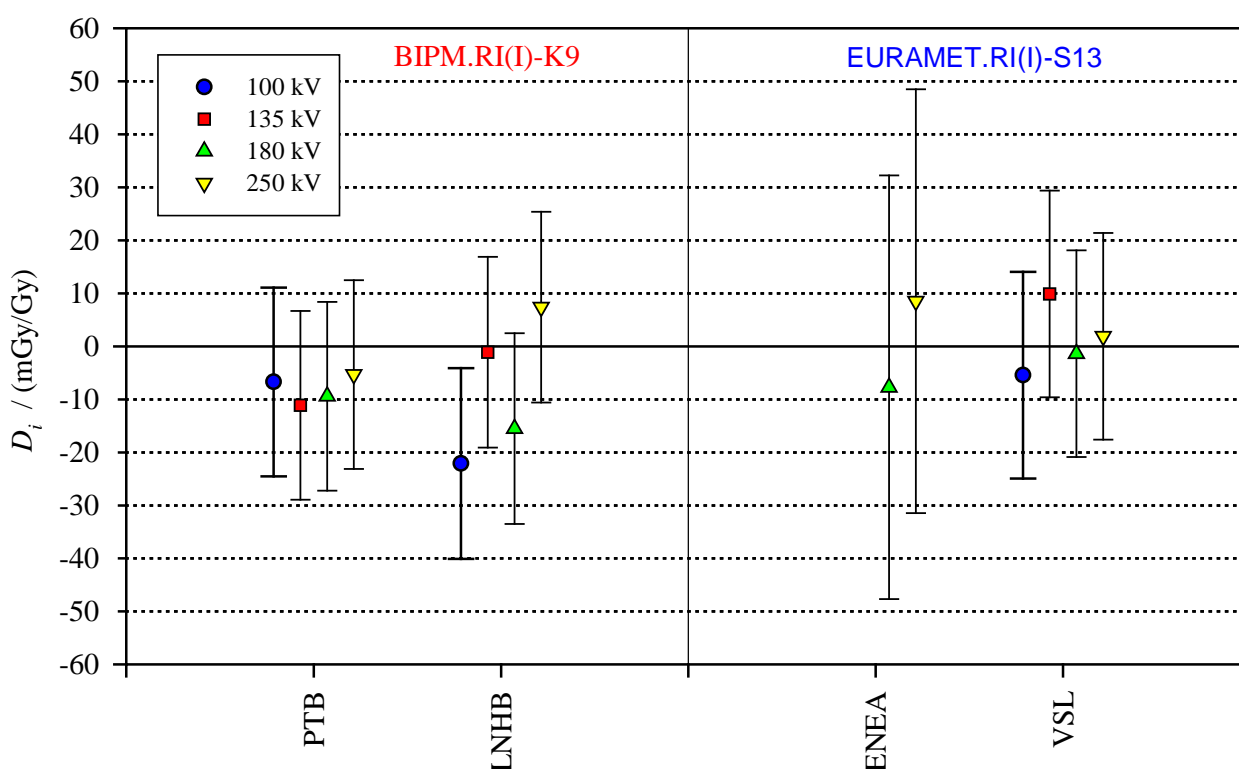
Figure 2. Degrees of equivalence for each laboratory *i* with respect to the key comparison reference value. Results to the left of the line are for the ongoing international comparison BIPM.RI(I)-K9 and those to the right for the regional comparison EURAMET.RI(I)-S13.

12. Conclusions

The key comparison BIPM.RI(I)-K9 for the determination of absorbed dose to water in medium-energy x-rays shows the standards of the LNE-LNHB and the BIPM to be in general agreement at the level of the expanded ($k = 2$) uncertainty of the comparison of 2 parts in 10^2. Tables and graphs of degrees of equivalence, including those for the corresponding EURAMET.R(I)-S13 comparison, are presented for entry in the BIPM key comparison database.

References

Boutillon M 1978 Mesure de l'exposition au BIPM dans le domaine des rayons X de 100 à 250 kV *Rapport BIPM*-78/3

Büermann L, Guerra A S, Pimpinella M, Pinto M, de Pooter J, de Prez L, Jansen B, Denoziere M and Rapp B 2016 First international comparison of primary absorbed dose to water standards in the medium-energy x-ray range *Metrologia* **53** *Tech. Suppl.* 06007

Burns D T 2003 Degrees of equivalence for the key comparison BIPM.RI(I)-K3 between national primary standards for medium-energy x-rays *Metrologia* **40** *Tech. Suppl.* 06036

Burns D T 2004 Changes to the BIPM primary air-kerma standards for x-rays *Metrologia* **41** L3

Burns DT 2017 The correction factors $k_{ii}k_W$ for free-air chambers *Rapport* CCRI(I)/17-08

Burns D T and Kessler C 2009 Diaphragm correction factors for free-air chamber standards for air kerma in x-rays *Phys. Med. Biol.* **54** 2737–45

Burns D T and Kessler C 2018 Re-evaluation of the BIPM international dosimetry standards on adoption of the recommendations of ICRU Report 90 *Metrologia* **55** R21–26

Burns D T, Kessler C and Roger P 2017 New BIPM absorbed-dose standard for medium-energy x-rays *Rapport* CCRI(I)/2017-06

CCEMRI 1972 Qualités de rayonnement *Comité Consultatif pour les Étalons de Mesures des Rayonnements Ionisants (Section I)* 2nd *meeting* R15–16

ICRU 2016 Key data for ionizing-radiation dosimetry: Measurement standards and applications *J. ICRU* **14** Report 90 (Oxford University Press)

KCDB 2019 The BIPM key comparison database is available online at http://kcdb.bipm.org/

Rapp B, Perichon N, Denoziere M, Daures J, Ostrowsky A and Bordy J-M 2013 The LNE-LNHB water calorimeter for primary measurement of absorbed dose at low depth in water: application to medium-energy x-rays *Phys. Med. Biol.* **58** 2769–86